C. R. Acad. Sci. Paris, Ser. I 352 (2014) 761–766

Contents lists available at ScienceDirect

C. R. Acad. Sci. Paris, Ser. I

www.sciencedirect.com

Mathematical problems in mechanics

A hybrid collocated/staggered version of the Fast Vector Penalty-Projection method for dilatable fluids

Une version hybride colocalisée/décalée de la méthode Fast Vector Penalty-Projection pour les fluides dilatables

Michel Belliard

Commissariat à l'énergie atomique et aux énergies alternatives (CEA), DEN/DANS/DM2S/STMF/LMEC, CEA Cadarache, bât. 238, 13108 Saint-Paul-lez-Durance, France

ARTICLE INFO

Article history:
Received 29 January 2014
Accepted 15 May 2014
Available online 12 August 2014

Presented by Olivier Pironneau

ABSTRACT

We propose a hybrid version of the Fast VPP method for dilatable fluids: collocated variables/staggered projection. The necessary conditions for its effective application are outlined. Numerical results illustrate the significant computation-cost reduction to reach stationary regimes.

RÉSUMÉ

On propose une version hybride de la méthode Fast-VPP en écoulement dilatable : variables colocalisées et projection décalée. On précise les conditions nécessaires à son application efficace. Des résultats numériques illustrent le gain en effort de calcul pour l'obtention de régimes stationnaires.

Version française abrégée

La méthode *Fast Vector Penalty-Projection* [1,2] permet de résoudre les équations de Navier–Stokes (Eqs. (1)–(4)) pour un fluide incompressible. Un petit paramètre de pénalité $0 < \epsilon \ll 1$ contrôle la conservation de la masse. Son principal intérêt réside dans une résolution extrêmement rapide de l'étape de projection. À notre connaissance, la mise en œuvre des Eqs. (5)–(7) n'a été faite qu'en variables décalées. On propose ici une version volumes finis hybride de la Fast VPP pour des écoulements dilatables, cf. Eqs. (9)–(11). Les variables restent colocalisées, cf. Eqs. (13)–(14), mais la projection est faite en variables décalées, à l'instar de [5] pour le schéma de Chorin–Temam. Après avoir exposé les discrétisations spatiale et temporelle concernant l'étape de projection, cf. Eq. (15), on analyse les propriétés de la matrice correspondante. En particulier, son noyau n'est pas réduit au seul élément nul et elle n'est pas forcément à dominance diagonale $\forall\epsilon$. Ceci a des conséquences sur le solveur linéaire utilisé pour la résolution. On indique les conditions nécessaires à l'application efficace de la méthode ILU(0)–BiCGStab, en particulier la détermination d'un ϵ_{opt} optimal, cf. Eq. (17). Des résultats numériques

E-mail address: michel.belliard@cea.fr.

http://dx.doi.org/10.1016/j.crma.2014.05.004
1631-073X/

illustrent l'efficacité de cette approche, qui permet de réduire sensiblement l'effort de calcul du terme de pression pour la simulation de régimes stationnaires. Ceci est tout particulièrement vrai dans le cas d'un grand nombre de degrés de liberté.

1. Introduction

We propose a hybrid version of the Fast Vector Penalty-Projection (VPP) method, see [1,2], in the framework of the Finite Volume (FV) method using collocated variables on Cartesian grids for dilatable fluids. The most attractive feature of the fast VPP is its capability to easily solve the projection step in comparison with the classical Chorin–Temam method [4,7]. The Navier–Stokes equations for a Newtonian fluid in Ω, an open of $\mathbb{R}^d$, $d = 2, 3$, are:

$$\partial_t \rho + \nabla \cdot (\rho \mathbf{v}) = 0 \quad \text{in } \Omega \times [0, T] \tag{1}$$

$$\partial_t (\rho \mathbf{v}) + \nabla \cdot (\mathbf{q} \otimes \mathbf{v}) + \nabla P - \nabla \cdot \tau(\mathbf{v}) = \mathbf{g} \quad \text{in } \Omega \times [0, T] \tag{2}$$

$$+ \text{boundary conditions for } \rho,\ \mathbf{v} \text{ and } P \quad \text{on } \partial\Omega \times [0, T] \tag{3}$$

$$+ \text{initial conditions for } \rho,\ \mathbf{v} \text{ and } P \quad \text{in } \Omega \text{ at } t = 0 \tag{4}$$

with ρ the density, P the pressure, $\mathbf{v}$ the fluid velocity, $\mathbf{q} = \rho\mathbf{v}$ the mass flux, $\tau(\mathbf{v}) = \mu((\mathbf{grad} + \mathbf{grad}^{\mathrm{T}})\mathbf{v} - \frac{2}{3}\operatorname{div}\mathbf{v}\, I)$ the viscous strain and μ the dynamic viscosity. At the semi-discrete level, the incremental form of the VPP scheme for incompressible fluids reads as [1]:

$$\frac{\tilde{\mathbf{v}}^{n+1} - \mathbf{v}^n}{\Delta t} + \frac{1}{\rho} DC\big(\mathbf{v}^n, \tilde{\mathbf{v}}^{n+1}\big) = -\frac{1}{\rho}\nabla P^n + \frac{\mathbf{g}^{n+1}}{\rho} \tag{5}$$

$$\epsilon\left(\frac{\hat{\mathbf{v}}^{n+1}}{\Delta t} + \frac{1}{\rho} DC\big(\mathbf{v}^n, \hat{\mathbf{v}}^{n+1}\big)\right) - \nabla\big(\nabla \cdot \hat{\mathbf{v}}^{n+1}\big) = \nabla\big(\nabla \cdot \tilde{\mathbf{v}}^{n+1}\big) \tag{6}$$

$$\frac{1}{\rho}\phi^{n+1} = -\frac{1}{\epsilon}\nabla \cdot \mathbf{v}^{n+1} \tag{7}$$

where Δt is the time step, DC the semi-discrete form of the diffusion–convection operator from Eq. (2), $\hat{\mathbf{v}}^{n+1} := \mathbf{v}^{n+1} - \tilde{\mathbf{v}}^{n+1}$, $\phi^{n+1} = P^{n+1} - P^n$ and $0 < \epsilon \ll 1$ the penalty parameter. For Eq. (5), the boundary conditions (BC) are taken from (3). BCs for $\hat{\mathbf{v}}$ are homogeneous Dirichlet conditions where the velocity is prescribed. Thanks to Eq. (7), it is possible to recover the pressure. This suggests also homogeneous Dirichlet conditions for $\nabla \cdot \mathbf{v}$ where the pressure is prescribed. In fact, it is not useful to reconstruct the pressure at each time step. We can use Eqs. (6) and (7) to update the pressure gradient: $\nabla P^{n+1} = \nabla P^n + \nabla\phi^{n+1}$.

The VPP method shares some links with the augmented Lagrangian [6] and the artificial compressibility methods [3], see [1]. Eq. (7) is similar to $\frac{1}{\rho}\phi^{n+1} = -r\nabla \cdot \mathbf{v}^{n+1}$ with an augmentation parameter $r = \frac{1}{\epsilon}$. Angot et al. have proven the convergence of the velocity divergence $|\nabla \cdot \mathbf{v}|_{L^2}$ with the order $\mathcal{O}(\epsilon)$ for a given Δt [1].

At the semi-discrete level, the Fast version of the VPP scheme consists in replacing Eq. (6) by [2]:

$$\frac{\epsilon}{\Delta t}\hat{\mathbf{v}}^{n+1} - \nabla\big(\nabla \cdot \hat{\mathbf{v}}^{n+1}\big) = \nabla\big(\nabla \cdot \tilde{\mathbf{v}}^{n+1}\big) \tag{8}$$

Unlike the VPP scheme, the fast one does not provide a semi-discrete form of Eq. (2) under the constraint (7). But its main interest is to be found in the easily solving of Eq. (8). With a small enough value for the penalty parameter $\frac{\epsilon}{\Delta t}$, the right-hand side of this linear system is formed using the same matrix than the left-hand side. If we denote by W the matrix associated with the operator $\nabla(\nabla \cdot *)$, we have: $\hat{\mathbf{v}}^{n+1} = \frac{\Delta t}{\epsilon}(I - \frac{\Delta t}{\epsilon}W)^{-1}W\tilde{\mathbf{v}}^{n+1}$ and $\hat{\mathbf{v}}^{n+1} \approx -W^{-1}W\tilde{\mathbf{v}}^{n+1}$ for $0 < \frac{\epsilon}{\Delta t} \ll 1$. Using an iterative solver for this linear system, we can take advantage of this feature by an appropriated preconditioning as the ILU one. Lets notice that the W matrix is a non-symmetric one and we have to choose the iterative solver under this constraint. Here we consider the BiCGStab iterative method.

Hereafter, we detail our FV hybrid collocated/staggered version for dilatable fluids on Cartesian grids and give some numerical illustrations showing the capacity of our approach to effectively reduce the computational cost to reach stationary regimes.

2. A hybrid collocated/staggered Fast VPP

At the semi-discrete level, the proposed incremental form of the Fast VPP scheme for dilatable fluids (or variable-density flows) reads as:

$$\frac{\tilde{\mathbf{q}}^{n+1} - \mathbf{q}^n}{\Delta t} + DC\big(\rho^{n+1}, \mathbf{v}^n, \tilde{\mathbf{v}}^{n+1}\big) = -\nabla P^n + \mathbf{g}^{n+1} \tag{9}$$

$$\frac{\epsilon}{\Delta t}\hat{\mathbf{q}}^{n+1} - \nabla\big(\nabla \cdot \hat{\mathbf{q}}^{n+1}\big) = \nabla\left(\nabla \cdot \tilde{\mathbf{q}}^{n+1} + \frac{\rho^{n+1} - \rho^n}{\Delta t}\right) \tag{10}$$

$$\nabla\phi^{n+1} = -\frac{\hat{\mathbf{q}}^{n+1}}{\Delta t} \tag{11}$$

where $\mathbf{q}^{n+1} := \rho^{n+1}\mathbf{v}^{n+1}$, $\tilde{\mathbf{q}}^{n+1} := \rho^{n+1}\tilde{\mathbf{v}}^{n+1}$ and $\hat{\mathbf{q}}^{n+1} := \rho^{n+1}\hat{\mathbf{v}}^{n+1} = \mathbf{q}^{n+1} - \tilde{\mathbf{q}}^{n+1}$. Let's remark that this system differs from the one given in [1] for a generalization to variable-density flows: $\rho^{n+1}\frac{\tilde{\mathbf{v}}^{n+1}-\mathbf{v}^n}{\Delta t} + \ldots = -\nabla P^n + \mathbf{g}^{n+1}$ and $\frac{\epsilon}{\Delta t}\hat{\mathbf{q}}^{n+1} - \nabla(\nabla\cdot\hat{\mathbf{v}}^{n+1}) = \nabla(\nabla\cdot\tilde{\mathbf{v}}^{n+1})$. The evolution of the density is supposed to be given by an extra balance equation; for instance, the energy balance equation equipped with the equation of state $\rho(e)$. Confronting Eq. (10) with Eq. (11), we get an equation involving ϕ and $\hat{\mathbf{q}}$, that is similar to Eq. (7):

$$\phi^{n+1} = -\frac{1}{\epsilon}\left[\nabla\cdot\mathbf{q}^{n+1} + \frac{\rho^{n+1}-\rho^n}{\Delta t}\right] \tag{12}$$

It can be viewed as a particular form of artificial compressibility applied to the constraint $\nabla\cdot\mathbf{q} = -\frac{\rho^{n+1}-\rho^n}{\Delta t}$.

We consider a FV space discretization with collocated variables (density, velocity, mass flux, and pressure) at the cell centers of a Cartesian grid. Hereafter, we denote by K a cell and σ a cell face. Notation $*_K$ or $*_\sigma$ will stands for a cell or a face variable, respectively. The VPP method was successfully tested with a staggered-variable scheme on structured [1] or unstructured [2] meshes. For staggered-variable schemes, the FV approximation of the $\nabla\cdot\mathbf{q}$ operator is located at the cell centers—denoted $\nabla_K\cdot\mathbf{q}_\sigma$—and all the needed data are available: $\mathbf{q}_\sigma\cdot\mathbf{n}_\sigma$ with $\mathbf{n}_\sigma$ the face normal. The FV approximation of the $\nabla(*)$ operator—denoted $\nabla_\sigma(*_K)$—is located at the face centers. It gives the correction field for which only the normal components $\hat{\mathbf{q}}_\sigma\cdot\mathbf{n}_\sigma$ are useful and the BCs well defined.

Using the VPP method with collocated variables is not so easy. For collocated-variable schemes, the $\nabla\cdot*$ operator is approximated at the face centers $\nabla_\sigma\cdot*_K$ and the $\nabla(*)$ one at the cell centers $\nabla_K(*_\sigma)$. There is no problem defining the latter operator $\nabla_K(*_\sigma)$, but it is not the case for the former one $\nabla_\sigma\cdot*_K$. Indeed, we have no specification for the boundary conditions concerning the needed tangential velocities: the term $\frac{\partial q_\tau}{\partial\tau}$ with τ the boundary tangent. Here, we overcome this issue using a hybrid collocated/staggered solver for which the projection step is done on the cell faces. In fact, it was already the case in the FV scheme presented by Faure et al. [5]. The hybrid method that we propose applies a collocated-variable scheme for the predicted velocity step and a staggered-variable scheme for the projection step.

The cell-center velocities $\tilde{\mathbf{v}}_K$ verify the momentum balance equation using convection fluxes $\mathbf{q}_\sigma = \rho_\sigma\mathbf{v}_\sigma$ at the face centers:

$$|K|\frac{\rho_K^{n+1}\tilde{\mathbf{v}}_K^{n+1} - \rho_K^n\mathbf{v}_K^n}{\Delta t} + \sum_{\sigma\in\epsilon(K)}|\sigma|\tilde{\mathbf{v}}_\sigma^{n+1}\mathbf{q}_\sigma^n\cdot\mathbf{n}_\sigma - D_K\left(\tilde{\mathbf{v}}_K^{n+1},\tilde{\mathbf{v}}_L^{n+1}\right) = -\nabla_K P_K^n + |K|\,\mathbf{g}_K^{n+1} \tag{13}$$

with $\epsilon(K)$ the faces of the cell K, $|*|$ the measure of K or σ, $D_K(*)$ a space-time discretization of the diffusion term (with cells L in the vicinity of K) and $\tilde{\mathbf{v}}_\sigma$ given by an appropriate interpolation. The normal components of the convection fluxes $\mathbf{q}_\sigma\cdot\mathbf{n}_\sigma$ verify the mass balance equation (and not the $\rho_K\mathbf{v}_K$ themselves):

$$|K|\frac{\rho_K^{n+1}-\rho_K^n}{\Delta t} + \sum_{\sigma\in\epsilon(K)}|\sigma|\mathbf{q}_\sigma^{n+1}\cdot\mathbf{n}_\sigma = 0 \tag{14}$$

Hence, the corrections $\hat{\mathbf{q}}$ live on σ and we only need the normal components $\hat{\mathbf{q}}_\sigma\cdot\mathbf{n}_\sigma$ given by the normal dot product of Eq. (10). Lets $\tilde{\mathbf{q}}_\sigma^{n+1} = \rho_\sigma^{n+1}\tilde{\mathbf{v}}_\sigma^{n+1}$ be a mass flux prediction involving appropriate face interpolations of ρ_K and $\tilde{\mathbf{v}}_K$ on σ. Then, we consider the following FV approximation of the normal dot product of Eq. (10):

$$\frac{\epsilon}{\Delta t}\hat{\mathbf{q}}_\sigma^{n+1}\cdot\mathbf{n}_\sigma - \nabla_\sigma\left(\frac{\nabla_K\cdot\hat{\mathbf{q}}_\sigma^{n+1}}{|K|}\right)\cdot\mathbf{n}_\sigma = \nabla_\sigma\left(\frac{\nabla_K\cdot\tilde{\mathbf{q}}_\sigma^{n+1}}{|K|} + \frac{\rho_K^{n+1}-\rho_K^n}{\Delta t}\right)\cdot\mathbf{n}_\sigma \tag{15}$$

In this equation, the cell divergence and the normal face gradient are defined by linear interpolations (but higher-order interpolations can be used): $\nabla_K\cdot*_\sigma = \sum_{\sigma\in\epsilon(K)}|\sigma|*_\sigma\cdot\mathbf{n}_\sigma$ and $\nabla_\sigma(*_K)\cdot\mathbf{n}_\sigma = \frac{*_K-*_L}{h_\sigma}$. Here K and L are the cells sharing the face σ and such that $\mathbf{n}_\sigma$ is directed from K to L and h_σ is the normal distance between the K and L cell centers. As a consequence, Eq. (15) gives only access to the normal components of $\hat{\mathbf{q}}_\sigma$. As already mentioned, the BCs for this quantity are well defined. When the normal inflow mass flux is imposed ($\tilde{\mathbf{q}}_\sigma\cdot\mathbf{n}_\sigma = \mathbf{q}_{\sigma_{BC}}\cdot\mathbf{n}_\sigma$), we have $\hat{\mathbf{q}}_\sigma\cdot\mathbf{n}_\sigma = 0$. And when the outflow pressure is imposed ($P_\sigma = P_{\sigma_{BC}}$; $\phi_\sigma = 0$), we get $(\nabla\cdot\mathbf{q} + \frac{\partial\rho}{\partial t})_\sigma = 0$ from Eq. (12).

Once $\hat{\mathbf{q}}_\sigma^{n+1}\cdot\mathbf{n}_\sigma$ is obtained from Eq. (15), the normal components of the cell-face mass flux are updated: $\mathbf{q}_\sigma^{n+1}\cdot\mathbf{n}_\sigma = \tilde{\mathbf{q}}_\sigma^{n+1}\cdot\mathbf{n}_\sigma + \hat{\mathbf{q}}_\sigma^{n+1}\cdot\mathbf{n}_\sigma$. Similarly, Eq. (11) provides the update of the normal component of the cell-face pressure gradient $\nabla_\sigma(P_K^{n+1})\cdot\mathbf{n}_\sigma = \nabla_\sigma(P_K^n)\cdot\mathbf{n}_\sigma - \frac{\hat{\mathbf{q}}_\sigma^{n+1}}{\Delta t}\cdot\mathbf{n}_\sigma$. But, for the collocated cell-centered FV scheme used with the momentum balance equation, we need to update the cell quantities. Hence, we define the following linear interpolation of the components: $\hat{\mathbf{q}}_K^{n+1}\cdot\xi = \frac{\hat{\mathbf{q}}_{\sigma^+}^{n+1}\cdot\mathbf{n}_{\sigma^+} - \hat{\mathbf{q}}_{\sigma^-}^{n+1}\cdot\mathbf{n}_{\sigma^-}}{2}$, where ξ is the unitary vector in the considered component direction and σ^+ (resp. σ^-) a cell

face of K such as $\mathbf{n}_{\sigma^+} = \xi$ (resp. $\mathbf{n}_{\sigma^-} = -\xi$). Then, we update the cell mass flux by $\mathbf{q}_K^{n+1} = \tilde{\mathbf{q}}_K^{n+1} + \hat{\mathbf{q}}_K^{n+1}$, the cell velocity by $\mathbf{v}_K^{n+1} = \frac{\mathbf{q}_K^{n+1}}{\rho_K^{n+1}}$ and the cell pressure gradient by:

$$\nabla_K P_K^{n+1} = \nabla_K P_K^n - \frac{\hat{\mathbf{q}}_K^{n+1}}{\Delta t} \tag{16}$$

The properties of the non-symmetric matrix $[\frac{\epsilon}{\Delta t} - \nabla_\sigma(\frac{\nabla_K \cdot}{|K|})]$, denoted by $\frac{\epsilon}{\Delta t} I - W$, result from the linear approximations of the operators $\nabla_K \cdot$ and ∇_σ. As its Kernel is not reduced to the single $\{\mathbf{0}\}$, spurious waves may occur without stabilization process (not discussed here). Moreover, as $\sum_{i \neq j} |a_{(i,j)}| = 10/h^2$ and $|a_{(i,i)}| = 2/h^2 + \epsilon/\Delta t$, the matrix $\frac{\epsilon}{\Delta t} I - W$ is a non-diagonal dominant one unless $\frac{\epsilon}{\Delta t}$ is big enough. Here, i and j stand for the row and column indexes (two tabular-index triplets) and $a_{(i,j)}$ for the matrix coefficients. We can determine an optimal value for the penalty parameter $\frac{\epsilon}{\Delta t}$ in order to get a diagonal-dominant matrix $\frac{\epsilon}{\Delta t} I - W$. In the limit $\frac{\epsilon}{\Delta t} \approx 0$, the above equations show that the sum of the absolute values of the extra-diagonal terms is $r_a = 5$ times bigger than the diagonal term itself. Hence we can determine $\delta a_{(i,i)} = \frac{\epsilon_{\text{opt}}}{\Delta t}$ in such a way that this ratio would be the unity: $|a_{(i,i)} + \frac{\epsilon_{\text{opt}}}{\Delta t}| = \sum_{i \neq j} |a_{(i,j)}| = r_a |a_{(i,i)}|$. This relation leads to $\epsilon_{\text{opt}} = (r_a - 1) \max|a_{(i,j)}| \, \Delta t$ that is:

$$\epsilon_{\text{opt}} \approx 8 \max\left\{\frac{1}{h_x^2}, \frac{1}{h_y^2}, \frac{1}{h_z^2}\right\} \Delta t. \tag{17}$$

Obviously ϵ_{opt} no more verifies $0 < \epsilon \ll 1$. Indeed, this approach is relevant to the class of the augmented Lagrangian methods [6] with an augmented Lagrangian term $r\nabla(\partial_t \rho + \nabla \cdot \mathbf{q})$ and $0 < r = \frac{1}{\epsilon_{\text{opt}}}$.

3. An example of numerical application

Our purpose is not to widely check our proposed hybrid scheme but only to provide a very first insight into its application to dilatable fluids computed with collocated variables on Cartesian grids. Our test case consists in a 2D stationary dilatable vortex flow (computed in 3D). The 3D computational domain Ω is a cube of length one, centered in $(-0.5, -0.5, 0.5)^{\mathrm{T}}$. The stationary regime is found by a time marching algorithm in $[0, T]$:

$$\partial_t w + \nabla \cdot (w\mathbf{v}) = 0 \quad \text{in } \Omega \times [0, T] \tag{18}$$

$$\partial_t \rho\mathbf{v} + \nabla \cdot (\rho\mathbf{v} \otimes \mathbf{v}) - \nabla \cdot \tau(\mathbf{v}) + \nabla P = \mathbf{0} \quad \text{in } \Omega \times [0, T] \tag{19}$$

$$\rho(x, y, z) = (\rho_1 - \rho_0) w(x, y, z) + \rho_0 \quad (\text{EOS};\ \rho_0 = 1 \text{ and } \rho_1 = 2). \tag{20}$$

The stationary analytical solution is: $w(x, y, z) = \frac{1}{2}(x^2 + y^2)$, $\mathbf{v}(x, y, z) = (-y, x, 0)^{\mathrm{T}}$ and $P(x, y, z) = \frac{1}{8}(x^2 + y^2)^2 + \frac{1}{2}\rho_0(x^2 + y^2) + P_0$ with for instance $P_0 = 0$. This solution is a polynomial one of degree two in w and ρ, of degree one in $\mathbf{v}$ and of degree four in P. And we have $\nabla \cdot \mathbf{v} = 0$. At the inflow, we prescribe Dirichlet BC for w and $\mathbf{v}$ and homogeneous Neumann one for P. At the outflow, we prescribe Dirichlet BC for P and Neumann ones for w and $\mathbf{v}$. The transposed part of the stress tensor ($\mu = 10^{-3}$) is not considered here.

The system of Eqs. (18)–(20) is solved in there steps. The first one is devoted to the computation of w_K^{n+1}, ρ_K^{n+1} and the interpolation ρ_σ^{n+1}. With the second one, we obtain a predicted velocity $\tilde{\mathbf{v}}_K^{n+1}$ and the interpolation $\tilde{\mathbf{v}}_\sigma^{n+1}$. Finally, the correction mass flux $\hat{\mathbf{q}}_\sigma^{n+1}$ is computed as well as the corrected mass flux $\mathbf{q}_\sigma^{n+1}$, the interpolated corrected velocity $\mathbf{v}_K^{n+1}$ and the interpolated corrected pressure gradient $\nabla_K P_K^{n+1}$. Given an initial guess $\nabla_K P_K^0$, the pressure gradient is straightforwardly obtained from Eq. (16). (In the case of the Chorin–Temam scheme, $\nabla_K P_K := \sum_{\sigma \in \epsilon(K)} |\sigma| P_\sigma \mathbf{n}_\sigma$, where P_σ is computed through an interpolation of the directly available pressure P_K.)

As a whole, the Fast VPP scheme produces quantitatively similar results to those of the Chorin–Temam scheme. Table 1 gives a compilation of the results obtained with the linear interpolations for the operators $\nabla_K \cdot$ and ∇_σ, the upwind scheme for the convection of $\mathbf{v}$ and of w. The accuracy and the space convergence order $\mathcal{O}(h^1)$ of the errors in the L^2 and L^∞ norms are kept for the w and the $\mathbf{v}$ variables. This latter point is also true for the L^2 norm of the pressure-gradient error. But the pressure boundary layers are larger than those obtained with the Chorin–Temam scheme. It limits the pressure-gradient error convergence order in L^∞ norm. Lets notice that substituting the linear interpolation formula to compute $\hat{\mathbf{q}}_K^{n+1}$ by a quadratic formula is a way to increase the smoothness of the pressure-gradient error distribution and to reduce the magnitude of the pressure boundary layers.

As claimed in [1] for incompressible flows, ϵ provides a control on the L^2 norm of the velocity divergence. The decrease in the velocity divergence error is controlled by an $\mathcal{O}(\epsilon \Delta t)$ term. Here, we can expect a similar behavior for the mass balance error $|\partial_t \rho + \nabla \cdot \mathbf{q}|_{L^2}$. Using a fixed time step, Fig. 1(a) illustrates this point for the L^∞ norm. Once ϵ is small enough, this error is drastically reduced in a linear way. The number of unpreconditioned BiCGStab iterations to solve the linear system is quite large: e.g., at time step number two, about 75, whatever ϵ is. The Chorin–Temam algorithm needs about the same number of Conjugate Gradient (CG) iterations for this time step. Moreover, the BiCGStab method requires two matrix vector products by iteration instead of only one for the CG. Hence, preconditioning is required. Using the maximal pivot

Table 1
Absolute errors and space convergence orders in L^2 and L^∞ norms for the Fast VPP projection scheme using linear interpolations for the operators $\nabla_K \cdot$ and ∇_σ. Comparison with the Chorin–Temam projection scheme. Upwind scheme for the convection of $\mathbf{v}$ and of w. Linear interpolation for $\hat{\mathbf{q}}_K^{n+1}$. CFL = 0.25. Grids $10 \times 10 \times 5$ and $20 \times 20 \times 5$: 800 Δt; $40 \times 40 \times 5$: 1500 Δt.

Grid	$\lvert e_w \rvert_{L^2}$ (ratio)	$\lvert e_w \rvert_\infty$ (ratio)	$\lvert e_{\mathbf{v}} \rvert_{L^2}$ (ratio)	$\lvert e_{\mathbf{v}} \rvert_\infty$ (ratio)	$\lvert e_{\nabla P} \rvert_{L^2}$ (ratio)	$\lvert e_{\nabla P} \rvert_\infty$ (ratio)	Scheme
$10 \times 10 \times 5$	$3.88 \cdot 10^{-2}$	$7.58 \cdot 10^{-2}$	$2.64 \cdot 10^{-2}$	$4.37 \cdot 10^{-2}$	$1.63 \cdot 10^{-1}$	$5.73 \cdot 10^{-1}$	Fast VPP
$20 \times 20 \times 5$	$2.18 \cdot 10^{-2}$ (1.78)	$4.89 \cdot 10^{-2}$ (1.55)	$1.39 \cdot 10^{-2}$ (1.90)	$2.81 \cdot 10^{-2}$ (1.56)	$8.12 \cdot 10^{-2}$ (2.01)	$3.52 \cdot 10^{-1}$ (1.63)	Fast VPP
$\hat{\mathbf{q}}_K^{n+1}$ quadratic interpolation	$2.18 \cdot 10^{-2}$	$5.30 \cdot 10^{-2}$	$1.39 \cdot 10^{-2}$	$3.12 \cdot 10^{-2}$	$3.73 \cdot 10^{-2}$	$1.96 \cdot 10^{-1}$	
$40 \times 40 \times 5$	$1.19 \cdot 10^{-2}$ (1.83)	$2.93 \cdot 10^{-2}$ (1.67)	$7.33 \cdot 10^{-3}$ (1.90)	$1.38 \cdot 10^{-2}$ (2.04)	$3.44 \cdot 10^{-2}$ (2.36)	$3.32 \cdot 10^{-1}$ (1.06)	Fast VPP
$10 \times 10 \times 5$	$3.88 \cdot 10^{-2}$	$7.61 \cdot 10^{-2}$	$2.56 \cdot 10^{-2}$	$4.29 \cdot 10^{-2}$	$1.42 \cdot 10^{-1}$	$6.42 \cdot 10^{-1}$	Chorin–Temam
$20 \times 20 \times 5$	$2.19 \cdot 10^{-2}$ (1.77)	$4.91 \cdot 10^{-2}$ (1.55)	$1.38 \cdot 10^{-2}$ (1.86)	$2.80 \cdot 10^{-2}$ (1.53)	$6.40 \cdot 10^{-2}$ (2.22)	$3.46 \cdot 10^{-1}$ (1.86)	Chorin–Temam
$40 \times 40 \times 5$	$1.14 \cdot 10^{-2}$ (1.92)	$2.80 \cdot 10^{-2}$ (1.75)	$7.21 \cdot 10^{-3}$ (1.91)	$1.53 \cdot 10^{-2}$ (1.83)	$2.89 \cdot 10^{-2}$ (2.21)	$1.94 \cdot 10^{-1}$ (1.78)	Chorin–Temam

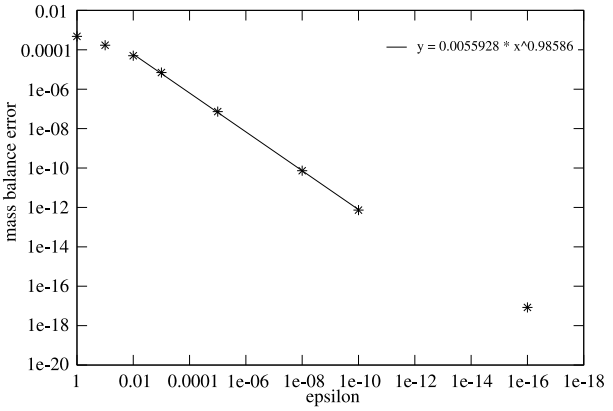

(a) Mass balance error in L^∞ norm versus ϵ. Time step number two. Upwind scheme for the convection of w.

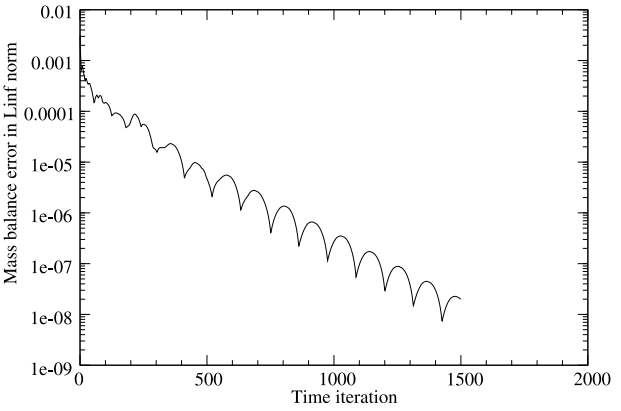

(b) ILU(0)-preconditioned BiCGStab method: mass balance error in L^∞ norm versus the iteration number. $\epsilon = 25.28$. QUICK scheme for the convection of w.

Fig. 1. Fast VPP mass balance errors. Linear interpolations for the operators $\nabla_K \cdot$ and ∇_σ. Upwind scheme for the convection of $\mathbf{v}$. Grid $20 \times 20 \times 5$. CFL = 0.25. $\Delta t \approx 8 \cdot 10^{-3}$ s.

algorithm to compute the ILU(0) preconditioning matrix, we get small values for some diagonal entries—around 10^{-12}—leading to the computation failure. Choosing the optimal values ϵ_{opt}, we recover a diagonal-dominant matrix. For instance, with the grid $20 \times 20 \times 5$ and $\Delta t = 5.6 \cdot 10^{-3}$ s, a numerical application of Eq. (17) gives $\epsilon_{\text{opt}} \approx 17.9$ and $r = \frac{1}{\epsilon_{\text{opt}}} \approx 6 \cdot 10^{-2}$. In this case, the smallest diagonal entry of the ILU(0) matrix is about 10^{-1}. The discretization errors at the end of the transient (stationary regime) are identical whatever the used iterative method (ILU(0)–BiCGStab or BiCGStab). However, the mass balance residual, controlled by Eq. (12), is relatively high (10^{-3} to 10^{-4}) at the beginning of the transient, but quickly decreases during the transient (ϕ^{n+1} is nul for the steady state), cf. Fig. 1(b).

The number of BiCGStab iterations is amazingly reduced with the ILU(0) preconditioning. Indeed, the transient-averaged number of ILU(0)–BiCGStab is independent of the grid resolution: about 3 whatever the grid size, instead of 27.7 ($10 \times 10 \times 5$) to 191.5 ($80 \times 80 \times 5$) BiCGStab iterations for the Chorin–Temam scheme. Concerning the transient CPU time, the speed-up of the overall computation is between about 1.6 (coarsest grid) and 2.7 (finest grid) in comparison with the Chorin–Temam computation.

References

[1] P. Angot, J.-P. Caltagirone, P. Fabrie, Vector Penalty-Projection methods for the solution of unsteady incompressible flows, in: Finite Volumes for Complex Applications V, Aussois, France, Wiley, 8–13 June 2008, pp. 169–176.
[2] P. Angot, J.-P. Caltagirone, P. Fabrie, A spectacular Vector Penalty-Projection method for Darcy and Navier–Stokes problems, in: Finite Volumes for Complex Applications VI, Prague, Czech Republic, Wiley, 1–23 July 2011.
[3] A.J. Chorin, A numerical method for solving incompressible viscous flow problems, J. Comput. Phys. 2 (1967) 12–26.
[4] A.J. Chorin, Numerical solution of the Navier–Stokes equations, Math. Comp. 22 (1968) 745–762.

[5] S. Faure, J. Laminie, R. Temam, Colocated finite volume schemes for fluid flows, Commun. Comput. Phys. 4 (1) (2008) 1–25.
[6] M. Fortin, R. Glowinski, Augmented Lagrangian Methods: Applications to the Numerical Solution of Boundary-Value Problems, Studies in Mathematics and Its Applications, vol. 15, North-Holland, Amsterdam, 1983.
[7] R. Temam, Sur l'approximation de la solution des équations de Navier–Stokes par la méthode des pas fractionnaires, Arch. Ration. Mech. Anal. 32 (1969) 135–153.